NIST-GCR-91-590

Sprinkler/Hot Layer Interaction

FILE COPY
DO NOT REMOVE

Gunnar Heskestad

Factory Mutual Research Corp.
1151 Boston-Providence Turnpike
Norwood, MA 02062

Sponsored by:
U.S. DEPARTMENT OF COMMERCE
National Institute of Standards
and Technology
Building and Fire Research Laboratory
Gaithersburg, MD 20899

U.S. DEPARTMENT OF COMMERCE
Robert A. Mosbacher, Secretary
NATIONAL INSTITUTE OF STANDARDS
AND TECHNOLOGY
John W. Lyons, Director

NIST

NIST-GCR-91-590

Sprinkler/Hot Layer Interaction

Gunnar Heskestad

Factory Mutual Research Corp.
1151 Boston-Providence Turnpike
Norwood, MA 02062

September 1990

Issued May 1991

NIST Grant No. 60NANBOD1006

Sponsored by:
U.S. DEPARTMENT OF COMMERCE
National Institute of Standards and Technology
Building and Fire Research Laboratory
Gaithersburg, MD 20899

U.S. DEPARTMENT OF COMMERCE
Robert A. Mosbacher, Secretary
NATIONAL INSTITUTE OF STANDARDS AND TECHNOLOGY
John W. Lyons, Director

Notice

This report was prepared for the Building and Fire Research Laboratory of the National Institute of Standards and Technology under Grant Number 60NANB0D1006. The statements and conclusions contained in this report are those of the authors and do not necessarily reflect the views of the National Institute of Standards and Technology or the Building and Fire Research Laboratory.

TECHNICAL REPORT

SPRINKLER/HOT LAYER INTERACTION

by

Gunnar Heskestad

Factory Mutual Research Corporation

1151 Boston-Providence Turnpike

Norwood, Massachusetts 02062

Prepared for:

U.S. Department of Commerce

National Institute of Standards and Technology

Center for Fire Research

Grant No. 60NANB0D1006

FMRC J.I. OT1N2.RU

070(A)

September 1990

Approved by:

Cheng Yao

Cheng Yao
Vice President & Manager
Research Division

Factory Mutual Research

1151 Boston-Providence Turnpike
Norwood Massachusetts 02062

ABSTRACT

A model has been developed for the cooling of a quiescent hot layer by a sprinkler spray in a two-layer zone model (with no direct interaction of the spray with a fire plume), based on existing models of spray-induced flow and heat transfer to evaporating drops. In addition, existing models have been adapted to predict the penetration of the spray-induced flow below the layer interface and associated entrainment of lower-layer fluid into the upper layer. The cooling model is in good agreement with published results from sprinklered room-fire experiments, for which penetration of spray-induced flow into the lower layer and associated entrainment were calculated to be negligible. No published results have been found to test the validity of the adapted models of penetration and associated entrainment, which do not account for possible effects of the spray below the layer interface.

TABLE OF CONTENTS

Section	Title	Page
ABSTRACT		iv
ACKNOWLEDGMENTS		vii
I	INTRODUCTION	1
II	ELEMENTS OF MODEL	5
	2.1 Entrainment into Water Spray	5
	2.2 Penetration of Spray Induced Flow into Lower Layer	11
	2.3 Entrainment of Lower Layer Fluid into Upper Layer	13
	2.4 Heat Transfer to Evaporating Liquid Drops	16
	2.5 Heat Balance in Upper Layer	18
III	VERIFICATION AND CALIBRATION OF MODEL	21
	3.1 Available Experiments	21
	3.2 Verification of Cooling Model	27
IV	PENETRATION AND ENTRAINMENT BEHAVIOR	36
V	MODEL PARAMETERS	40
VI	CONCLUSIONS	41
REFERENCES		42
SYMBOLS		44

LIST OF FIGURES

Figure	Title	Page
1	Entrainment of gas from hot layer by discharging sprinkler and formation of vertical jet.	2
2	Penetration of spray induced jet into lower layer, accompanied by entrainment from lower layer.	3
3	Replot of Turner's data on upward rise (penetration) of salt-water jets injected into fresh water.	12
4	Test facility employed by You et al.[14]	22
5	Freeburn temperature profiles in centerplane of room opening[16] in experiments reported by You et al.[14,15]	25
6	Temperature profiles in centerplane of room opening for tests with $Q_s/Q_a = 0.55$ and smaller[16] in experiments reported by You et al.[14,15]	26
7	Ratios $\zeta = d_c/d$ indicated by experiments of You et al.[14], plotted as a function of the heat release rate.	33
8	Comparison of calculated and experimental[14] spray cooling rates.	35
9	Influence of the temperature difference between gas in spray and lower layer on jet penetration depth beneath layer interface for various layer depths, δ_u.	37
10	Volumetric entrainment rates from lower layer associated with Figure 9.	38

LIST OF TABLES

Table	Title	Page
I	Numerical Solutions for Entrainment in Conical Sprays[2]	7
II	Nondimensional Drop Velocities Associated with the Calculations in Table I	8
III	Conditions[16] For Tests Conducted by You Et Al.[14,15]	23
IV	Trial Calculation of Gas and Drop Velocities in Sprinkler Spray of Test 23	30

ACKNOWLEDGMENTS

The author acknowledges the contributions of Dr. Leonard Y. Cooper, Center for Fire Research, NIST Scientific Officer for this grant, who proposed this study and the conceptual approach. He is indebted to Dr. Hong-Zeng Yu, who made available data from his files to supplement published information referenced in this report.

FACTORY MUTUAL RESEARCH CORPORATION

LIST OF FIGURES

Figure	Title	Page
3	Effect of Turner's data on smoke rise (pollutant) in lower jets injected into fresh water.	23
4	Test facility employed by Yu et al.[18]	25
5	Pressure (momentum) profiles in centerplane of cycle 1 (A,18) opening[18] in experiments reported by Yu et al.	27
6	Temperature profiles in centerplane of room opening for cycle with Q_{in} = 0.55 and position[18] in experiments reported by Yu et al.[18,19]	28
7	Ceiling ϕ i.e. ϕ_c indicated by experiments of Yu et al.[18] plotted as a function of the heat release rate.	31
8	Comparison of calculated and experimental[18] spray cooling rates.	35
9	Influence of the temperature difference between jet in spray and lower layer on jet penetration depth beneath layer interface for various layer depths, h_{∞}.	37
10	Volumetric entrainment rates from lower layer associated with Figure 9	38

LIST OF TABLES

Table	Title	Page
I	Numerical Solutions for Turbulent Jet in Conical Spray[17]	7
II	Nondimensional Drop Velocity Corresponding with the Calculations in Table I	8
III	Conditions[18] for Tests Conducted by Yu et al.[18,19]	22
IV	Trial Calculation of Gas and Drop Velocities in Cardioid Spray of Test 23	40

I

INTRODUCTION

The objective of this program has been to develop a submodel for sprinkler/hot layer interactions to be incorporated in a two-layer zone model of compartment fires.

In fire tests conducted within the large volume of the Factory Mutual Research Corporation test building in West Glocester, RI, the smoke layer (hot, upper layer) underneath the ceiling has been observed in numerous tests to remain well stratified during the active phase of a fire. However, smoke has been observed to penetrate into the clear air, especially during smoky fires. This penetration forms as pockets beneath sprinklers operating away from the immediate fire plume. It is clear that the smoke is pulled down by the action of the water droplets and returned to the smoke layer by buoyancy. A turbulent, churning motion is evident in the penetration pockets. Operation of the last sprinkler in a test usually signals that the sprinklers have gained control of the fire and gas temperatures under the ceiling are beginning to fall rapidly. Soon afterward smoke is transported completely to the floor by the operating sprinklers as buoyancy decays, and smoke is rapidly dispersed throughout the test volume.

In the two-layer zone model of the objective, it is visualized that there is an upper layer of hot fire gases of uniform temperature under the ceiling of the compartment and a lower layer of relatively cool gases of uniform temperature extending to the floor. A single sprinkler operates near the ceiling within the upper layer. The spray entrains hot gases from the upper layer, producing a vertical jet toward the layer interface, Figure 1. The gases in the jet have increased water content and reduced temperature relative to the quiescent hot layer because of evaporation of water drops. After the jet penetrates the interface, it is surrounded by cool air and experiences an upward, buoyant force which eventually reverses the downward flow back into the upper layer, in the process entraining air from the lower layer, Figure 2. The basic information required includes the evaporation rate of water and the mass transfer rate from the lower layer to the upper layer, from which the contribution to cooling of, and mass addition to the upper layer can be calculated.

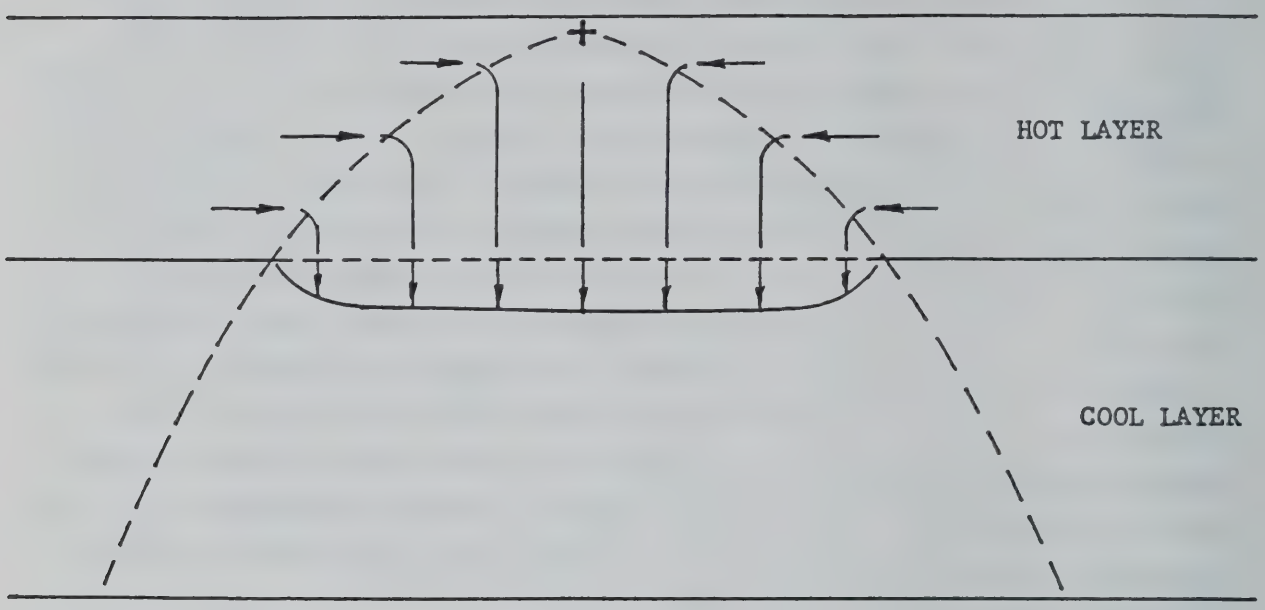

Figure 1. Entrainment of gas from hot layer by discharging sprinkler and formation of vertical jet.

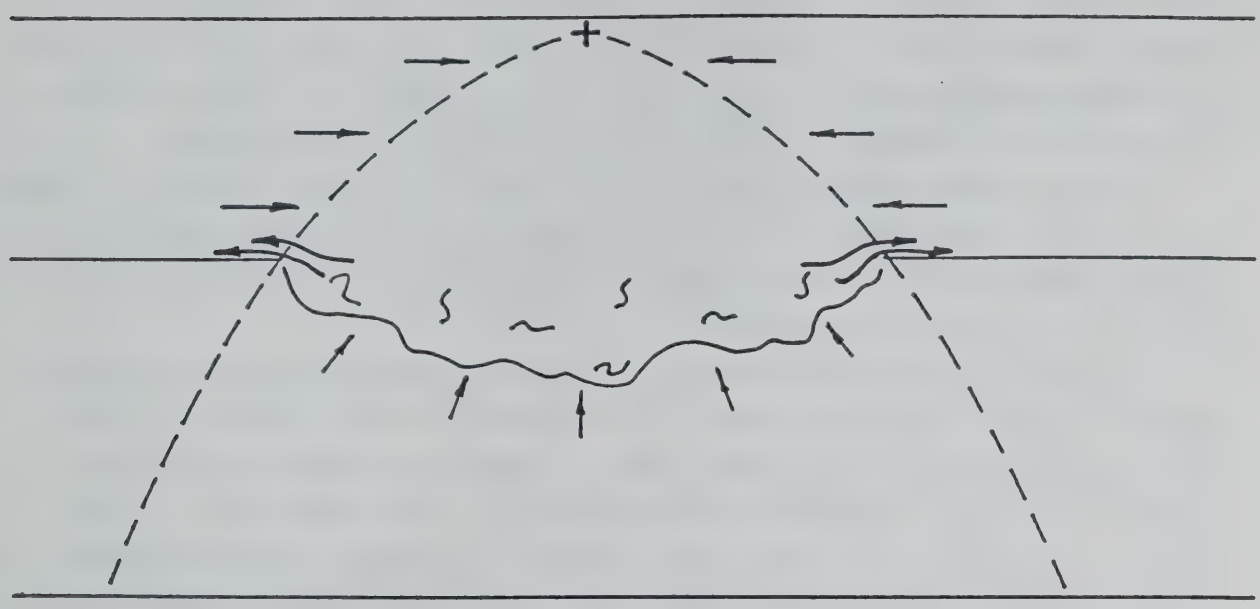

Figure 2. Penetration of spray induced jet into lower layer, accompanied by entrainment from lower layer.

Entrainment of gas (air) into a water spray has been treated by Heskestad et al.[1,2]. Penetration of a jet across a density interface has been investigated by Turner[3], and entrainment of fluid of the penetrating jet into the layer from which it projects from the other side of the density interface, has been studied by Baines.[4] Finally, Yuen and Chen[5] have established heat-transfer correlations for evaporating liquid drops which make it possible to calculate evaporation and cooling rates. In this report the various pieces are adapted and assembled to produce the required prediction methods.

For sprinklers operating near the fire source, one should ideally account for the direct interaction with the fire plume as well, including additional cooling and penetration of water drops to the base of the fire. The present work did not consider such effects.

Elements of the problem under study have previously been investigated by others. Bullen[6] proposed a model for assessing the likelihood of a sprinkler discharge causing a hot smoke layer to break up and form a plume down into the clear area, involving the downward drag of the aggregate of drops versus the buoyancy of the hot layer. Morgan[7] proposed a tentative model for heat transfer to a sprinkler spray from a hot layer, based on heat transfer to a single water drop as it describes its trajectory, which he subsequently compared with a few experimental results.[8] On the basis of Morgan's model, Heselden[9] derived an empirical equation for the heat absorption rate of a sprinkler spray, also quoted by Hinkley[10].

II

ELEMENTS OF MODEL

2.1 ENTRAINMENT INTO WATER SPRAY

A one-dimensional theory for entrainment of air into water sprays discharging vertically downward in a quiescent, isothermal environment has been derived and experimentally verified by Heskestad et al.[1,2]. The essential features of the theory include a prescribed spray boundary and momentum exchange between the water drops and the entrained air.

The theory leads to the following set of coupled differential equations for the drop velocity and air velocity in the spray.

$$du_p^*/dx^* = (\xi/\beta)^4 u_p^{*-1} - \beta u_p^{*-1} (u_p^* - u^*)^{3/2} \tag{1}$$

$$du^*/dx^* = - u^* x^{*-1} + \gamma\beta x^{*-2} (u_p^* u^*)^{-1} (u_p^* - u^*)^{3/2} \tag{2}$$

with the initial conditions that at $x^* = (2 \tan\theta)^{-1}$, $u^* = u_p^* = 1$,
where:

$u_p^* = u_p/u_{po}$, nondimensional drop velocity
$u^* = u/u_{po}$, nondimensional air velocity
$x^* = x/D_w$, nondimensional axial distance
u_{po} = initial drop velocity
D_w = effective initial spray diameter

The initial drop velocity is calculated from:

$$u_{po} = C_M [\dot{V}_w/(\pi D^2/4)] \tag{3}$$

where C_M is a momentum coefficient, defined as the initial momentum of the spray to the momentum of the water flow in the spray nozzle; $\dot{V}_w$ is the volumetric discharge rate of water from the nozzle; and D is the nozzle diameter. Furthermore, the effective initial spray diameter is defined as:

$$D_w = C_M^{-1/2} D \tag{4}$$

The parameters γ, β and ξ in Eqs. (1) and (2) are nondimensional, defined according to:

$$\gamma = \frac{1}{8} \rho_w \rho^{-1} (\tan \frac{\theta}{2})^{-2} \tag{5}$$

$$\beta = (3/4\ B\nu^{1/2}\ \rho\rho_w^{-1}\ C_M^{-1}\ r^{-3/2}\ u_n^{1/2} \tag{6}$$

$$\xi = (3/4)\ B\nu^{1/2} \rho\rho_w^{-1}\ g^{1/4} C_M^{-13/8}\ r^{-3/2}\ D^{1/4} \tag{7}$$

This is a convenient set for independent study of effects of spray angle, θ (via γ), nozzle discharge velocity, u_n (via β), and nozzle diameter, D (via ξ). Other symbols include ρ_w, the water density; ρ, the air (gas) density; and g, the acceleration of gravity. The symbol r is a drop size parameter in the correlation equation:

$$d = r(D/u_n)^{2/3} \tag{8}$$

A value $r = 0.084\ m \cdot s^{-2/3}$ is typical of standard sprinklers when d is interpreted as the volume-mean diameter in the spray. The value $C_M = 0.4$ is representative of momentum coefficients of standard sprinklers[2]. B is a constant of proportionality related to aerodynamic drag of drops, given as 12.6.[2]

Table I presents tabulated values of nondimensional entrainment flow for a spray angle (at room temperature) of $\theta = 120°$ ($\gamma = 0.03445 \cdot 10^3$), taken from Reference 2. (Results are also presented for $\theta = 90°$, 60°, 30° in Ref. 2.) Nondimensional entrainment flow, Q*, is presented as a function of nondimensional vertical distance from the spray device, x*, at various combinations of β and ξ, where:

$$Q^* = \dot{V}_s / \dot{V}_w \tag{9}$$

Here, $\dot{V}_s$ is the total volumetric gas flow rate over a cross section of the water spray.

Table II presents nondimensional particle (drop) velocities associated with the results listed in Table I. These calculations have not been reported previously; they have been transcribed from the same computer printout from which Table I was constructed.[2]

OT1N2.RU

TABLE I

NUMERICAL SOLUTIONS FOR ENTRAINMENT IN CONICAL SPRAYS[2]

			Q* at x* indicated								
$\gamma \cdot 10^{-3}$	$\beta \cdot 10^{2}$	$\xi \cdot 10^{4}$	10	20	40	80	160	320	640	1280	2560
.03445	1	7.5	239	712	2,060	5,710	14,600	32,400	72,400	176,000	465,000
(120°)		15	239	713	2,070	5,770	15,100	37,900	99,300	272,000	761,000
		30	243	735	2,180	6,400	20,300	53,100	151,000	431,000	1,230,000
		60	283	899	2,820	8,730	26,700	80,000	236,000	681,000	1,950,000
	2	7.5	308	919	2,620	6,860	15,400	31,600	64,600	136,000	312,000
		15	308	919	2,620	6,870	15,500	33,200	75,400	189,000	516,000
		30	308	922	2,640	7,000	17,000	42,600	114,000	320,000	912,000
		60	314	956	2,830	8,150	23,100	65,600	187,000	535,000	1,520,000
	4	7.5	384	1,140	3,120	7,390	15,500	31,500	63,400	128,000	260,000
		15	384	1,140	3,120	7,390	15,500	31,600	64,700	137,000	317,000
		30	384	1,140	3,120	7,410	15,700	33,600	77,500	200,000	562,000
		60	385	1,140	3,150	7,690	18,100	46,400	128,000	367,000	1,070,000
	8	7.5	462	1,340	3,410	7,500	15,500	31,500	63,400	127,000	255,000
		15	462	1,340	3,410	7,500	15,500	31,500	63,400	128,000	260,000
		30	462	1,340	3,410	7,500	15,500	31,600	64,800	138,000	321,000
		60	462	1,340	3,410	7,530	15,800	33,900	79,100	199,000	599,000

TABLE II

NONDIMENSIONAL DROP VELOCITIES ASSOCIATED WITH THE CALCULATIONS IN TABLE I

			u_p^* at x^* indicated								
$\gamma \cdot 10^{-3}$	$\beta \cdot 10^2$	$\xi \cdot 10^4$	10	20	40	80	160	320	640	1280	2560
.03445	1	7.5	.943	.874	.735	.491	.177	.0503	.0366	.0306	.0275
(120°)		15	.948	.883	.755	.531	.266	.171	.157	.151	.147
		30	1.019	1.022	1.016	.493	.955	.920	.902	.892	.885
		60	1.81	2.31	2.99	3.80	4.64	5.27	5.53	5.54	5.54
	2	7.5	.905	.788	.569	.260	.0685	.0295	.0155	.0091	.0061
		15	.906	.789	.570	.263	.0758	.0415	.0291	.0232	.0201
		30	.910	.798	.589	.304	.149	.121	.110	.103	.098
		60	.981	.934	.843	.719	.636	.603	.586	.525	.567
	4	7.5	.852	.673	.389	.141	.0574	.0272	.0134	.0068	.0035
		15	.852	.673	.389	.142	.0578	.0280	.0146	.0083	.0054
		30	.852	.674	.391	.145	.0636	.0364	.0244	.0187	.0157
		60	.857	.683	.408	.181	.116	.0926	.0805	.0730	.0679
	8	7.5	.786	.550	.271	.116	.0544	.0265	.0131	.0065	.0033
		15	.786	.550	.271	.116	.0544	.0266	.0132	.0067	.0034
		30	.786	.550	.271	.116	.0547	.0272	.0141	.0079	.0049
		60	.786	.551	.272	.118	.0589	.0333	.0215	.0160	.0130

The results in Tables I and II, presented as functions of x^* for a given spray angle θ (120°), can alternatively be presented as functions of the non-dimensional radius, $R^* = R/D_w$, where $R = x \tan(\theta/2)$. If the tabulations for other spray angles are consulted[2], it is found that Q^* and u_p^* as functions of R^* are not very sensitive to the spray angle. Hence, Tables I and II can be used to predict entrainment and drop velocity for any spray angle likely to be encountered with automatic sprinklers, tying predictions to spray radius, rather than spray angle.

The particular association of spray angle θ with the parameter γ in Tables I and II has been calculated from Eq. (5), assuming room temperature air (ρ = 1.20 kg/m^3). At other temperatures the relation between γ and θ is obviously different, as is the relation between the spray radius R and the spray angle θ discussed in the preceding paragraph. If room temperature conditions are identified with subscript "o", it may be verified using Eq. (5) that the equation for spray radius in the preceding paragraph is generalized to elevated gas temperatures in the spray, T_s, according to:

$$R = x\,(T_s/T_o)^{1/2} \tan(\theta_o/2) \qquad (10)$$

The isothermal theory has to be assessed for effects of buoyancy forces in the application to sprinkler sprays discharging into a hot layer. Assuming a certain temperature of the gas phase in the spray, lower than the surrounding hot gas, one may calculate ratios of buoyancy forces to drag forces of the water drops, both tending to propel the entrained gas, building on elements of the existing theory. A specific case, considered previously in its isothermal version[1], has been calculated. This case involved a water discharge rate ($\dot{V}_w$) of $1.89 \cdot 10^{-3}$ m^3/s (30 gpm), an initial drop velocity (u_{po}) of 15 m/s, and a volume mean drop diameter (d) of 0.4 mm. At the position in the conical spray where the cross sectional area (A) was 0.66 m^2, the drop velocity (u_p) was 9 m/s and the air velocity (u_s) was 3.7 m/s. As a perturbation, we assume a surrounding hot gas (upper layer) temperature of T_u = 200°C and a gas temperature in the spray of T_s = 100°C. For this particular case, the ratio of buoyancy forces to drag forces is estimated at 0.10, sufficiently small so as not to be dominant in the process. Effects of other conditions may be assessed based on the following proportionality:

$$\frac{\text{Buoyancy forces}}{\text{Drag forces}} \propto \frac{A}{\dot{V}_w} \left(\frac{T_o}{T_s}\right)^{0.85} \frac{T_u - T_s}{T_u} \left[\frac{d}{(u_p - u_s)}\right]^{3/2} u_p \tag{11}$$

From this proportionality it is clear that buoyancy forces can become important in a continuously expanding spray. A tenfold increase in the cross-sectional area of the spray, not unrealistic in sprinkler applications, can make the buoyancy forces comparable to the drag forces. Effects on gas and drop velocities in the spray can be assessed from Eqs. (1) and (2), together with calculated results in Tables I and II and similar calculations for other values of γ. It is found for the case of a 120° spray (sprinkler-like) at $x^* = 80$, using typical values of β ($2 \cdot 10^{-2}$) and ξ ($30 \cdot 10^{-4}$), that including buoyancy forces equal to the drag forces increases the local entrainment flow rate by 28 percent and the local drop velocity by 18 percent. Effects of buoyancy forces are neglected in this investigation but might be included in future studies.

Other assumptions which are necessary in order to apply the existing entrainment predictions are 1) that evaporation of water is not sufficient to have a significant effect on the number density and size of the droplets propelling the entrained flow, and 2) that gas motion in the upper layer is not sufficient to invalidate the assumption that the surroundings of the spray are quiescent. With respect to the former assumption, it is sufficient to show (a posteriori) that the mass evaporation rate of water in the upper layer is small compared to the total discharge rate of water. With respect to the latter assumption, it is observed that significant motion in the upper layer will be confined to the ceiling jet generated by the fire plume, where velocities will typically be an order of magnitude smaller than the local drop velocities, which are expected to be close to their discharge value.

It is convenient to express the values of the spray parameters in Eqs. (1) - (3) in terms of their values at room temperature (20°C). If this is done it is found:

$$\beta = \beta_o \, (T_s/T_o)^{-0.15} \tag{12}$$

$$\xi = \xi_o \, (T_s/T_o)^{-0.15} \tag{13}$$

where β_o and ξ_o are calculated using room temperature. Instead of expressing γ in terms of γ_o, it is more useful to relate associated values tan $(\theta/2)$ and tan $(\theta_o/2)$:

$$\tan(\theta/2) = (T_s/T_o)^{1/2} \tan(\theta_o/2) \tag{14}$$

Hence, the value $\theta = 120°$ in Tables I and II refers to somewhat larger angles at elevated temperatures, as already implied in Eq. (10).

2.2 PENETRATION OF SPRAY INDUCED FLOW INTO LOWER LAYER

The penetration depth of a jet against opposing buoyancy forces into a fluid of different density has been studied by Turner.[3] In application to the problem at hand, the jet can be considered to be the flow entrained from the upper layer by the water spray, directed downward, whose characteristics are described by the jet velocity, width and excess temperature relative to the lower layer.

Turner studied the upward rise (penetration) of salt-water jets injected into fresh water. Using dimensional arguments, he predicted that the upward rise would be a linear function of a parameter formed from the momentum flux and buoyancy flux of the jet, assuming a point source. He plotted his experimental values of rise against this parameter for three nozzle sizes and demonstrated good linearity, as predicted. However, for small values of rise, the experimental points appear to deviate slightly from the adopted straight line fit, as if there were effects of finite nozzle sizes.

We decided to replot Turner's data on the assumption that effects of finite nozzle size could not be ruled out. The relationship sought was the nondimensional jet rise or penetration, δ_p/R, versus the nozzle Froude number, Fr, where δ_p is the jet rise, R is the nozzle radius, and:

$$Fr = u/[g(\Delta\rho/\rho_1)R]^{1/2} \tag{15}$$

In Eq. (15), u is the average nozzle velocity; $\Delta\rho$ is the density difference, salt water versus fresh water; and ρ_1 is the salt water density. Figure 3 presents the results of nondimensional rise versus Froude number for the three nozzle radii of the experiments, based on the data in Turner's Figure 5[3]

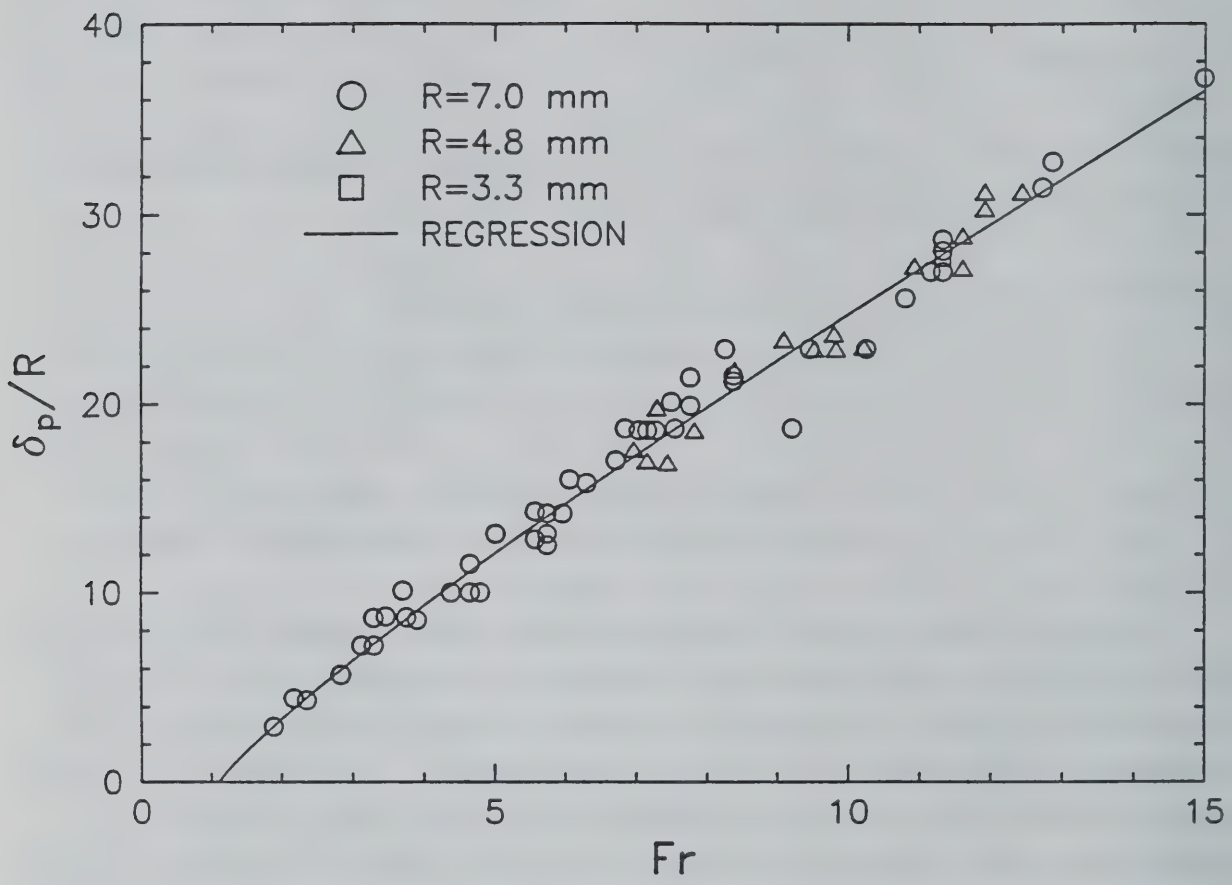

Figure 3. Replot of Turner's data on upward rise (penetration) of salt-water jets injected into fresh water, using nondimensional coordinates. Fr, defined in the text, is the Froude number at the injection nozzle.

(and corrections of the abscissa of that figure, communicated to us by Turner[11]). It is apparent, in this version of the data, that a minimum Froude number on the order of unity is required to produce jet penetration. The curve is a regression fit of the form $y = a\,(x-b)^n$, specifically:

$$\delta_p/R = 3.69\,(Fr - 1.1)^{0.870} \tag{16}$$

In adaptation to the interaction of sprinklers with hot layers, Eq. (16) may be written:

$$\delta_p/R_i = 3.69\,(Fr - 1.1)^{0.87} \tag{17}$$

where R_i is the spray radius at the level of the interface and

$$Fr = u_{si}/[g(\Delta T_s/T_\ell)\,R_i]^{1/2} \tag{18}$$

Here, u_{si} is the (uniform) gas velocity calculated in the spray at the level of the interface.

Although this adaptation of Turner's work[3] is appealing, it must be considered tentative. In the adaptation, the jet flow in the hot layer is generated by a spray whose effects have been ignored below the layer interface. The spray below the interface will entrain surrounding gas, which may affect the jet penetration. Furthermore, the spray produces a downward drag on the penetration, which is opposed by an upward buoyancy force on the penetrated fluid. Both of these forces are very nearly proportional to the penetration depth and, therefore, it is not clear what the net effect on the penetration depth will be.

2.3 ENTRAINMENT OF LOWER LAYER FLUID INTO UPPER LAYER

Baines[4] has investigated turbulent entrainment at a density interface like that between the upper and lower layer in the present problem. This entrainment refers to the entrainment of lower layer gas into the intruding jet from the upper layer, which reverses back into the upper layer.

In Baines' case, the density interface was produced in a tank by placing a layer of fresh water over a layer of salt water. Jet experiments were per-

formed with the aid of a small pipe producing a jet of fresh water against the density interface (from above), and plume experiments were performed substituting salt water for fresh water in the jet discharge. Dye was introduced into the jet to observe the entrainment process. Quoting from Baines[4]:

> "As the plume impinged on the interface it was observed to entrain fluid through its end over a relatively small area. This entrained fluid mixed with the plume fluid within a small volume, i.e., about the volume of a large eddy. Upon impact with the interface the large rotating lumps of fluid, i.e., the largest eddies, stopped their forward motion and moved out along the interface."

Baines found that a nondimensional volumetric entrainment rate could be expressed as a function of a Froude number, where the characteristic length, velocity and buoyancy were all associated with the plume or jet as it impinged on the density interface. His entrainment results can be expressed:

$$\frac{\dot{V}_e}{w_1 b_1^2} = 5.13 \cdot 10^{-2} Fr_G^3 \tag{19}$$

where $\dot{V}_e$ is the volumetric entrainment rate from the heavier layer; w_1 is the local centerline velocity (at impingement) of the plume or jet; b_1 is the local radius to 0.368 times the centerline velocity in the plume or jet, assuming a Gaussian profile; and the Froude number is defined:

$$Fr_G = \frac{w_1}{[g b_1 (\rho_2 - \rho_1)/\rho_{ao}]^{1/2}} \tag{20}$$

In the expression for the Froude number, ρ_2 is the density of the heavier fluid (salt water); ρ_1 is the local density on the plume or jet centerline; and ρ_{ao} is the density of the lighter fluid* (fresh water).

---

* Although Baines' Froude number is defined with ρ_{ao}, it is believed that ρ_1 is a more appropriate density at the location of ρ_{ao} in Eq. (20). Baines' correlation, Eq. (19), would not be affected significantly since ρ_{ao} and ρ_1 were of similar magnitudes in the experiments.

Baines' Froude number, Eq. (20) is based on variables of a Gaussian profile, while the Froude number in Eq. (15), used to correlate Turner's data in Figure 1, is based on plug flow in a tube. The two Froude numbers can be related, requiring that the two flow profiles have the same momentum flux, buoyancy flux, and total mass flow rate, so that;

$$u = \frac{1}{2} w_1 \; ; \; \Delta\rho/\rho_1 = \frac{1}{2} (\rho_2 - \rho_1)/\rho_{ao} ; \; R = 2^{1/2} b \tag{21}$$

with the consequence:

$$Fr_G = 2^{3/4} Fr \tag{22}$$

Baines[4] noted the depth of penetration into the heavy fluid layer, stating it "was barely perceptible at small $Fr_{[G]}$ but for $Fr_{[G]} > 2$, the plume or jet penetrated deeply." Using Eq. (22), the inequality $Fr_G > 2$ becomes $Fr > 1.2$, and Baines' observation then appears quite consistent with the interpretation of Turner's data[3] in Figure 3.

In terms of Fr, Eq. (19) becomes:

$$\frac{\dot{V}_e}{uR^2} = 0.244 \, Fr^3 \quad . \tag{23}$$

This form is compatible with the form of the induced flow predictions discussed in Section 2.1, which produce average values for the spray cross section. However, one more refinement is needed in application to the fire problem in recognition of the possibility that a large difference in density may exist between the upper and lower layers. In analogy with the work of Ricou and Spalding[12] on local entrainment rates in jets of different density than the surroundings, the mass entrainment rate across the interface is expected to obey:

$$\dot{m}_e \propto R \, (M\rho_\ell)^{1/2} \tag{24}$$

where M is the local momentum flux in the impinging jet. Substituting for M, one obtains:

$$\dot{m}_e \propto R^2 u(\rho_s \rho_\ell)^{1/2} \tag{25}$$

Hence, a suitable nondimensional entrainment rate is defined as:

$$\frac{\dot{m}_e}{uR^2(\rho_s\rho_\ell)^{1/2}} = \frac{\dot{m}_e/\rho_\ell}{uR^2\left(\frac{\rho_s}{\rho_\ell}\right)^{1/2}} = \frac{\dot{V}_e}{uR^2\left(\frac{T_\ell}{T_s}\right)^{1/2}}$$

Consequently, Eq. (23) is generalized to:

$$\frac{\dot{V}_e}{u_{si}R_i^2} = 0.244\left(\frac{T_\ell}{T_s}\right)^{1/2} Fr^3 \tag{26}$$

where $\dot{V}_e = \dot{m}_e/\rho_\ell$, the volumetric entrainment rate <u>from</u> the lower layer, and u and R have been replaced by u_{si} and R_i for application to the spray/hot layer problem in which case Fr is interpreted according to Eq. (18).

As cautioned at the end of the preceding section, there may possibly be effects of the spray traversing the penetrated fluid and of air entrained into the spray below the layer interface, which have not been accounted for in this treatment.

2.4 HEAT TRANSFER TO EVAPORATING LIQUID DROPS

Yuen and Chen[5] measured heat transfer to simulated (porous sphere) water and methanol droplets in a vertical hot air tunnel and established a relationship for the Nusselt number in terms of the Reynolds number, Prandtl number, and mass transfer number. The following expression can be derived from their work for the convective heat transfer coefficient for evaporating water drops, using the approximation that the dynamic viscosity of air is proportional to the 0.7 power of temperature:

$$h = \frac{2 + 0.6\left[\dfrac{\rho_o(T_o/T_a)\,(u_p - u_a)\,d}{\mu_o(T_f/T_o)^{0.7}}\right]^{1/2}\left[\dfrac{C_p\,\mu_o}{k_o}\right]^{1/3}\left[\dfrac{T_f}{T_o}\right]^{-0.05}}{d\,k_o^{-1}\,(T_a/T_o)^{-0.85}\,(1 + f\,(T_a - T_r)^{1.19})} \tag{27}$$

where:

h = convective heat transfer coefficient for a drop

ρ_o = density of air at standard temperature and pressure (STP)

T_o = room temperature (20°C)

T_a = air temperature

u_p = particle (drop) velocity

u_a = air velocity

d = drop diameter

μ_o = dynamic viscosity of air at room temperature

T_f = $(T_u + T_p)/2$, film temperature

T_u = temperature of upper layer

T_p = drop temperature (equal to wet bulb temperature)

C_p = specific heat of air at constant pressure

k_o = thermal conductivity of air at room temperature

f = $1.16 \cdot 10^{-4}\ K^{-1.19}$, a constant

T_r = 273K, a reference temperature

The film temperatures, T_f, require knowledge of the wet bulb temperatures, T_p, given by Yuen and Chen[13] as a function of the air temperature, T_a:

T_a (°C)	T_p (°C)
100	33
200	50
400	70
600	85
800	90
1000	95

These values can be used to establish the following expression for the film temperature:

$$T_f(K) = 0.543\ (T_a(K) + 245) \tag{28}$$

This model for the convective heat transfer coefficient assumes that water drops contributing significantly to evaporation and cooling in the hot layer are in approximate thermodynamic equilibrium with the environment, i.e., all heat transferred to the drops is absorbed in vaporizing the drops.

2.5 HEAT BALANCE IN UPPER LAYER

Equation (27) becomes, after substitution for T_f from Eq. (28) and various constants, as well as substituting the subscript "s" for "a" to refer specifically to the gas phase in the spray:

$$h(kW/m^2 \cdot K) = \frac{5.16 \cdot 10^{-5} + 4.55 \cdot 10^{-3} \left[\frac{T_o}{T_s}\right]^{1/2} \left[\frac{T_o}{T_s + 245}\right]^{0.40} (u_p - u_s) d^{1/2}}{\left(1 + 1.16 \cdot 10^{-4} (T_s - 273)^{1.19}\right) \left[\frac{T_o}{T_s}\right]^{0.85} d} \qquad (29)$$

The heat transfer per drop in the spray is:

$$h \pi d^2 (T_s - T_p) \quad .$$

The drop generation rate is:

$$\dot{V}_w/(\pi d^3/6) = 6\, \dot{V}_w/(\pi d^3) \quad .$$

The drop transit time in the upper layer is:

$$(\delta_u - \delta_s)/u_p \quad .$$

Consequently, the heat absorbed by the water spray can be calculated from:

$$Q_s = h \pi d^2 (T_s - T_p) \frac{6}{\pi} \frac{\dot{V}_w}{d^3} \frac{(\delta_n - \delta_s)}{u_p}$$

$$Q_s = 6 \frac{\dot{V}_w}{d} \frac{(\delta_u - \delta_s)}{u_p} (T_s - T_p)\, h \qquad (30)$$

where h is given by Eq. (29).

The heat removed from upper layer gas entrained in the spray is equal to the sum of heat absorbed by the water drops and the heat absorbed by air entrained from the lower layer:

$$\dot{V}_{si} \quad \rho_o \left[\frac{T_o}{T_u}\right] C_p \, (T_u - T_s) = 6 \, \frac{\dot{V}_w}{d} \, \frac{(\delta_u - \delta_s)}{u_p} \, (T_s - T_p) \, h + \dot{m}_e \, C_p \, (T_s - T_\ell) \qquad (31)$$

with h given by Eq. (29) in terms of u_p, u_s and the drop diameter d. Equation (31) is solved for the temperature in the gas phase in the spray, T_s, assuming that this temperature is constant throughout the spray. The upper layer temperature is taken as the value <u>in the absence</u> of the spray. The quantities u_p, u_s, $\dot{V}_s$ and d are calculated with the aid of the methods in Section 2.1, and the mass flow entrained from the lower layer, $\dot{m}_e$, is calculated as described in Section 2.3. The heat absorbed by the spray is then obtained from Eq. (30) and the mass addition rate of water vapor to the upper layer is calculated from:

$$\dot{m}_{ev} = Q_s / L_w \qquad (32)$$

where L_w is the latent heat of vaporization of water (2260 kJ/kg).

The drop and gas velocities in the spray, u_p and u_s, vary with the distance from the sprinkler. In the heat balance calculations, values averaged over the distance form the sprinkler to the layer interface are employed.

It has been assumed so far that the drops in the spray are uniform in size, or at least can be represented by their volume mean diameter. Whereas the volume mean diameter can be justified for entrainment calculations[1,2], we have not been able to show that the volume mean diameter is the appropriate effective diameter for cooling calculations. However, the effective diameter for cooling, d_c, might well be proportional to the volume mean diameter, d:

$$d_c = \zeta d \qquad (33)$$

where ζ is the constant of proportionality, as yet not known.

In many cases the spray induced flow in the upper layer will not penetrate significantly into the lower layer, according to the model discussed in Section 2.2. However, in other cases significant penetration may occur. In cases with significant penetration depth, one may assume that the heat transfer coefficient, gas temperature and relative velocity between drops and gas are the same as their respective averages in the spray above the interface. The average drop transit time through the penetration pocket is assumed as $\eta\ \delta_p/u_p$, where η is a constant of perhaps 0.5, δ_p is the (maximum) depth of the penetration, and u_p is the average drop velocity above the interface. Then the revised form of Eq. (31) would have the following substitution for $(\delta_u - \delta_s)$: $(\delta_u - \delta_s + \eta\ \delta_p)$.

III

VERIFICATION AND CALIBRATION OF MODEL

3.1 AVAILABLE EXPERIMENTS

A series of 25 sprinklered room fires have been reported by You et al.[14,15] which are available for testing the cooling predictions of the model. The tests involved three (steady) heat release rates, three sizes of geometrically similar sprinklers, and three sprinkler discharge rates.

A plan view of the test room[14] is reproduced in Figure 4a, showing a fire source located near one end of the test room and a floor-to-ceiling opening at the opposite end. The (pendent) test sprinkler was mounted under the ceiling, near the end of the room with the fire source, with its deflector 0.10 m from the ceiling. The three available geometrically similar sprinklers had nozzle diameters of 11.1, 8.36 and 6.94 mm. A side view of the fire source[14] is reproduced in Figure 4b, a heptane spray fire generated by a set of four oil-burner nozzles. The nozzle assembly was shielded from direct sprinkler water impingement with a 3.1 mm thick steel plate. The total heat release rate of a fire and the convective heat loss through the room opening were determined by calorimetry of the fire gases rising from the room opening. With the additional measurements of heat losses to ceilings and walls and radiative losses through the room opening, it was possible to determine the heat absorption rate of the sprinkler spray.

The 25 tests conducted by You et al.[14,15] are listed in Table III; the full table has not been reported previously but has generously been made available by the authors[16] for the purpose of this study. The table lists the sprinkler diameter(D); the discharge rate ($\dot{V}_w$); time from ignition when the measurements began; the actual heat release rate (Q_a); the convective heat loss rate (Q_c); heat losses to ceiling and walls, and radiative losses to floor and room opening (Q_ℓ); the heat absorption rate of the water spray (Q_s); the distance from the ceiling to the neutral plane in the room opening (h_n); the centerplane bulk gas temperature rise of the hot flow in the door opening[15] (ΔT_b); and the ambient temperature (T_∞).

Three freeburn tests were conducted, i.e., Test 13 at a heat release rate of 134 kW, Test 17 at 246 kW, and Test 21 at 396 kW. It may be verified that the bulk temperature rise, ΔT_b, scales nearly as $Q_a^{2/3}$ for these tests, as

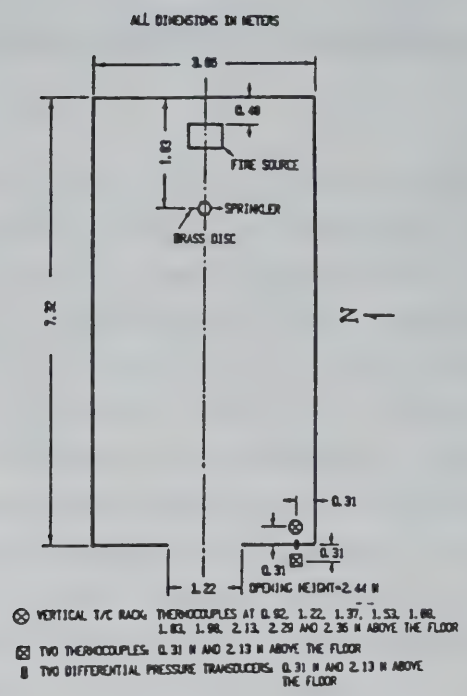

(a) Plan view of test room.

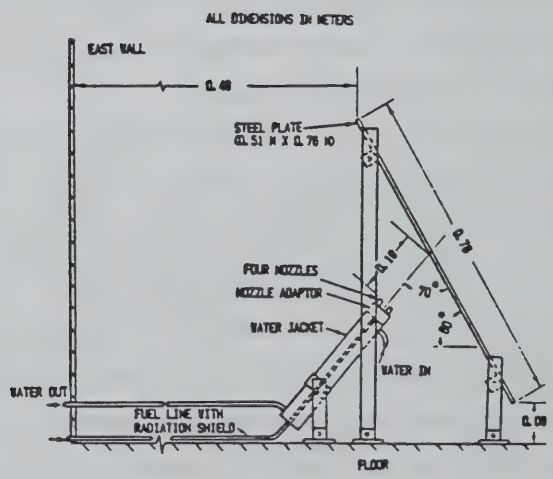

(b) Heptane spray fire source.

Figure 4. Test facility employed by You et al.[14]

TABLE III

CONDITIONS[16] FOR TESTS CONDUCTED BY YOU ET AL.[14,15]

Test No.	D (mm)	$\dot{V}_w$ (Liter/min)	Beginning of Investigation[a] Period (s)	Q_a (kW)	Q_c (kW)	Q_ℓ (kW)	Q_s (Kw)	h_n (m)	ΔT_b (°C)	T_∞ (K)
1	6.94	45.4	300	150	24.0	22.9	103.1	0.76	30	294
2	6.94	68.2	300	148	4.6	18.7	124.7	0.76	11	295
3	6.94	45.4	300	314	65.0	41.1	207.9	1.00	53	297
4	6.94	68.9	300	306	22.8	30.6	252.6	0.91	25	300
5	6.94	45.4	300	494	122.0	63.4	308.6	1.07	87	297
6	6.94	68.2	300	486	58.0	43.0	385.0	0.96	45	296
7	8.36	40.1	300	149	53.6	27.0	68.4	0.92	49	293
8	8.36	68.2	300	140	15.1	20.3	104.6	0.80	24	296
9	8.36	45.4	300	304	101.1	46.5	156.4	1.05	75	292
10	8.36	68.2	340	316	57.4	38.4	220.2	0.94	50	296
11	8.36	45.4	303	447	162.6	80.9	203.5	1.07	117	294
12	8.36	68.2	300	472	104.3	54.4	313.3	1.05	68	292
13	11.10	0	250	134	91.0	44.3	0	0.87	85	297
14	11.10	45.4	300	135	73.0	31.1	30.9	0.98	68	295
15	11.10	68.2	300	137	40.0	21.1	75.9	1.12	37	297
16	11.10	98.4	360	136	16.0	14.1	105.9	0.91	23	300
17	11.10	0	280	246	173.0	90.6	0	1.05	136	297
18	11.10	45.4	360	282	164.0	60.3	57.7	1.07	118	298
19	11.10	68.2	300	282	103.0	44.2	134.8	1.03	77	301
20	11.10	98.4	360	285	54.0	28.1	202.9	1.08	52	301
21	11.10	0	140	396	228.0	145.6	0	1.05	182	301
22	11.10	45.4	300	418	220.0	106.6	91.4	1.18	161	303
23	11.10	68.2	300	460	158.0	72.4	229.6	1.18	118	304
24	11.10	68.2	300	474	157.0	76.4	240.6	1.24	113	301
25	11.10	98.4	300	453	96.0	46.2	310.8	1.22	69	298

[a] timed from ignition.

expected based on known scaling rules.[17] Vertical temperature profiles[16] in the centerplane of the room opening for these tests are shown in Figure 5, presented as $\Delta T/\Delta T_b$ versus z/h_n, the latter being the distance from the ceiling normalized with the distance of the neutral plane from the ceiling. A fair approximation to a constant-temperature upper layer is evident, as represented by the dashed lines which define approximately the same integrated area as the actual temperature profile.

Among the sprinklered tests listed in Table III, a number of them produced temperature profiles in the room opening which can be considered to be of approximately constant temperature, as presented in Figure 6[16]. These tests included all the tests for which Q_s/Q_a was 0.55 or less. A number of tests with a ratio Q_s/Q_a of 0.65 or greater[16] produced approximately linearly decreasing $\Delta T/\Delta T_b$ with increasing z/h_n, reaching zero typically near z/h_n=1.5.

It was decided to limit analysis of sprinklered tests for the most part to cases with approximate two-layer temperature profiles, i.e., Tests 7, 9, 11 for the 8.36 mm nozzles and Tests 14, 15, 16, 18, 19, 20, 22, 23, 25 for the 11.10 mm nozzle. Among these, Tests 16 and 20 (with Q_s/Q_a values of 0.77 and 0.71) apparently did not produce approximate two-layer profiles. Test 24 was not included since it was a repeat of Test 23, with very similar results.

You et al. measured the volume median diameters,* d_m, of their three geometrically similar sprinklers at different water pressures[18] and found them to be correlated by an equation like Eq. (4):

$$d_m = 0.136\ (D/u_n)^{2/3} \tag{34}$$

Assuming a ratio of volume-median to volume-mean diameters of 2.1, as previously reported for a Rockwood T-4 nozzle[2], the coefficient r in Eq. (4), pertaining to the volume-mean diameter of the nozzles used in the experiments, becomes:

$$r = 0.065\ m \cdot s^{-2/3} \tag{35}$$

---

* The volume median diameter divides the drop population into equal volume fractions of smaller and larger drops.

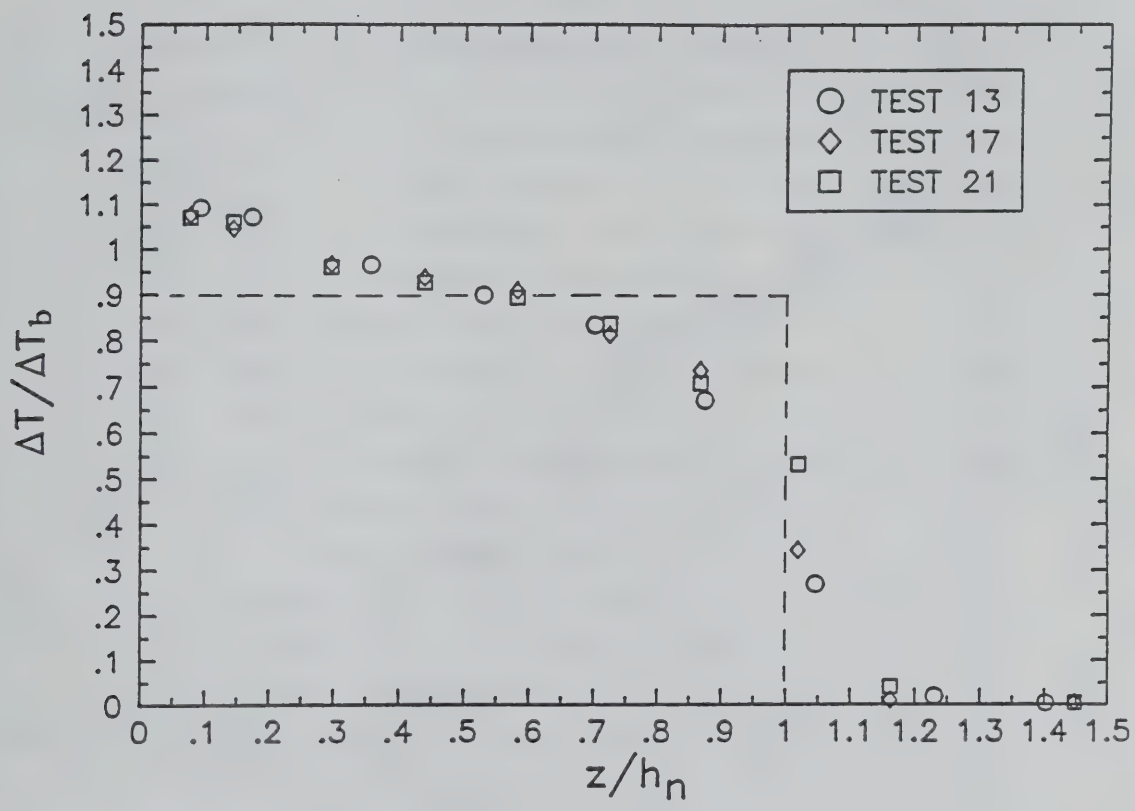

Figure 5. Freeburn temperature profiles in centerplane of room opening[16] in experiments reported by You et al.[14,15]

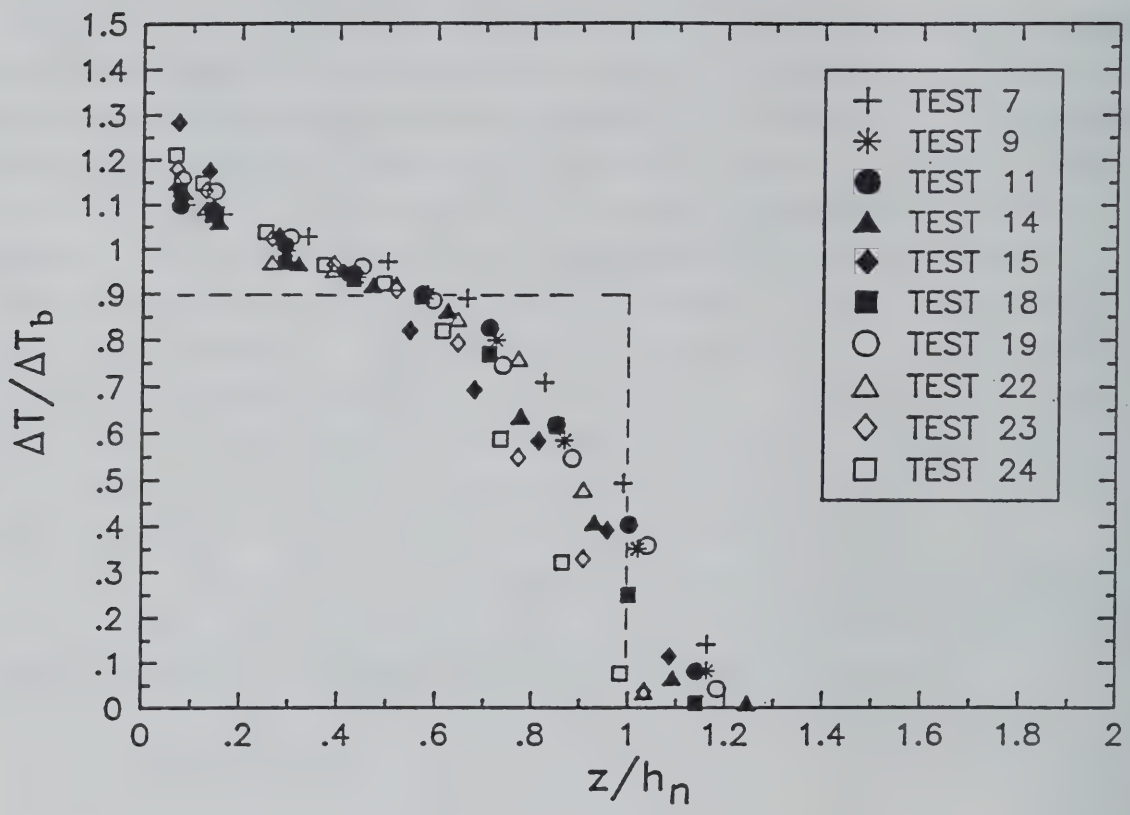

Figure 6. Temperature profiles in centerplane of room opening for tests with Q_s/Q_a = 0.55 and smaller[16] in experiments reported by You et al.[14,15]

This value is slightly smaller than the value 0.084 $m \cdot s^{-2/3}$ quoted after Eq. (4) as typical of standard sprinklers.

3.2 VERIFICATION OF COOLING MODEL

Verification of the cooling model will be investigated by comparing model predictions against the experiments summarized in the preceding section, in the following manner. For each experiment, the effective diameter for cooling introduced in conjunction with Eq. (33), d_c, will be calculated from the model so that the predicted cooling rate matches the measured cooling rate. It must then be shown that the associated fraction $\zeta = d_c/d$ [Eq. (33)] is approximately constant among the various experiments, where the volume-mean diameter, d, is calculated from Eq. (8). Using the value for r in Eq. (35), a realistic calibration for ζ is also established in this procedure.

First the properties of the hot layer in a two-layer representation is established. It is observed in Table III that the depths of the neutral plane, h_n, of the tests selected in the preceding section range from 1.0 to 1.2 m, including the freeburn tests. From Figures 5 and 6, the depth of the upper layer in a two-layer representation may be taken as $z/h_n = 1$, corresponding to actual depths, δ_u , in the range 1.0-1.2 m. An average depth δ_u = 1.1 m, will be assumed for all the selected tests. Referring to Figures 5 and 6 again, it is seen that a representative upper layer temperature corresponds to $\Delta T//\Delta T_b = 0.9$; actual values of temperature rise in the upper layer, ΔT_u, are then calculated as 0.9 ΔT_b, where ΔT_b is listed in Table III. For each sprinklered test, a value of the freeburn temperature at the heat release rate of the sprinklered test is needed. This temperature is determined using the freeburn test closest in heat-release rate to the sprinklered test, then adjusting the value ΔT_u, assuming $\Delta T_u \propto Q_a^{2/3}$ as justified in Section 3.1.

Calculation of the spray induced flow and drop velocities in the upper layer requires information on r, B and C_M (Section 2.1). The nominal values 0.084 $m \cdot s^{-2/3}$, 12.6 and 0.4 are selected, respectively. Although the nominal value for r, 0.084, is slightly larger than the best value available for the experiments* in Eq. (35), the difference is of little consequence for the

* The result in Eq. (35) was not available at the time the calculations were performed.

entrained flow calculations[1]. The typical value $C_M = 0.4$ is assumed because an experimental value is not available for the tested sprinklers. Other information required includes 1) the nozzle discharge velocity, u_n, calculated from the discharge rate and nozzle cross-sectional area; 2) the effective initial spray diameter, D_w, calculated from Eq. (7); and 3) the initial drop velocity, u_{po}, calculated from Eq. (9).

To proceed further, Test 23 is selected to illustrate procedure. Referring to Table III, this test involved a nozzle diameter D = 0.0111 m and a sprinkler discharge rate $\dot{V}_w = 68.2$ ℓ/min = $1.136 \cdot 10^{-3}$ m^3/s. The following quantities are calculated:

$$u_n = \dot{V}_w/(\pi D^2/4) = 1.136 \cdot 10^{-3}/ (\pi\ 0.0111^2/4) = 11.7 \text{ m/s}$$

$$D_w = C_M^{-1/2} D = 0.4^{-1/2} \cdot 0.0111 = 0.0176 \text{ m}$$

$$u_{po} = C_M\ [\dot{V}_w/(\pi D^2/4)] = 0.4 \cdot 11.7 = 4.68 \text{ m/s}$$

The parameter β may first be evaluated at room temperature, using Eq. (2) and $B = 12.6$, $\nu = 1.49 \cdot 10^{-5}$ m/s^2, $\rho = 1.2$ kg/m^3, $\rho_w = 1000$ kg/m^3, $C_M = 0.4$, $r = 0.084$, $u_n = 11.7$ m/s:

$$\beta_o = 1.54 \cdot 10^{-2}.$$

The parameter ξ at room temperature follows from Eq. (3):

$$\xi_o = 45.8 \cdot 10^{-4}$$

At the gas temperature in the spray, T_s, which is larger than room temperature, the values of β and ξ are smaller than β_o and ξ_o according to Eqs. (12) and (13). It is assumed for the present purpose that T_s can be set equal to the upper layer temperature, T_u, evaluated as described earlier in this section: $T_u = 126°C = 399K$. Hence $(T_s/T_o)^{-0.15} = 0.954$, so that:

$$\beta = 1.47 \cdot 10^{-2}$$
$$\xi = 43.7 \cdot 10^{-4}$$

Table IV lists Q^* and u_p^* as functions of x^* for the values of β and ξ just calculated, interpolated from Tables I and II and pertaining to a room temperature spray angle of 120°. The nondimensional parameters are converted to physical variables using Eqs. (5), (6) and (8). The spray radius corresponding to a given axial location x in the spray depends on the gas temperature in the spray, T_s, which is not known. However, as a first trial value the upper layer temperature determined for Test 23, T = 399K, is selected. The spray radius can then be calculated from Eq. (10) (using $\theta_o/2 = 60°$) and the gas velocity in the spray is determined from:

$$u_s = \dot{V}_s/\pi R^2 \tag{36}$$

It appears from spray distribution measurements[16] that the spray radius of the test sprinklers at the depth of the layer interface below the sprinklers, 1.1 - 0.1 = 1.0 m, is well represented by the radius of a 120° spray cone, which is 1.73 m. Hence, a location x is sought in the spray, represented in Table IV, where the spray radius is 1.73 m at the trial value of T_s. According to Eq. (10), this radius occurs at x = 0.856 m. The values of u_p and u_s for this location are determined by interpolation between x = 0.707 m and 1.408 m, and the associated value of $\dot{V}_s$ is obtained from $u_s(\pi R^2)$.

Penetration of the spray-induced jet into the lower layer and entrainment of lower-layer fluid into the upper layer may now be investigated, using the relations in Sections 2.2 and 2.3. There is no penetration and the entrainment rate of lower layer fluid is three orders of magnitude smaller than the flow rate, $\dot{V}_{si}$, associated with the spray induced jet at the layer interface.

With insignificant entrainment from the lower layer, the heat balance in Eq. (31) can be written in the convenient form:

$$b(T_u - T_s) = a\,(T_s - T_p) \tag{37}$$

where $$b = \dot{V}_{si}(\rho_o T_o/T_u)\,C_p \tag{38}$$

$$a = 6\,(\dot{V}_w/d)\,\left[(\delta_u - \delta_s)/u_p\right]h \tag{39}$$

TABLE IV

TRIAL CALCULATION OF GAS AND DROP VELOCITIES

IN SPRINKLER SPRAY OF TEST 23

($\beta = 1.47 \cdot 10^{-2}$; $\xi = 43.7 \cdot 10^{-4}$)

x^*	Q^*	u_p^*	x(m)	$\dot{V}_s$ $(\frac{m^3}{s})$	$u_p(\frac{m}{s})$	Trial T_s(K)	R(m)	u_s $(\frac{m}{s})$
10	284	1.05	0.176	0.322	4.95	399	0.355	0.813
20	869	1.02	0.352	0.987	4.81	399	0.711	0.621
40	2550	0.99	0.707	2.89	4.67	399	1.42	0.456
Int.	-	-	0.856	4.03	4.42	399	1.73	0.429
80	7340	0.75	1.408	8.34	3.54	399	2.84	0.329

$$T_{s2} = T_u - \frac{Q_s}{\dot{V}_{si}\rho_o(T_o/T_u)C_p} = 474 - \frac{230}{4.03 \cdot 1.2\ (293/474) \cdot 1.00} = 397K$$

(T_{s2} is essentially equal to first trial value of T_s, 399K; hence, T_s = 397 K.)

From Eq. (30) it is observed:

$$a(T_s - T_p) = Q_s \tag{40}$$

Combining Eqs. (37) and (40):

$$b(T_u - T_s) = Q_s \tag{41}$$

from which:

$$T_s = T_u - Q_s/b \tag{42}$$

Eq. (42), with substitution for b from Eq. (38), has been used at the bottom of Table IV to test the trial value of T_s (in terms of T_{s2}). Values of T_u and Q_s measured in the experiment are employed, together with the value of $\dot{V}_{si}$ resulting from the trial value of T_s, 4.03 m^3/s. It turns out that T_{s2} is essentially equal to the trial value in this case, so $T_s = T_{s2} = 397K$ is the final calculated value. If T_{s2} had not matched the trial value, it would have been employed as a second trial value and the procedure continued until convergence occurred.

The drop size which produces the correct cooling, Q_s, according to the model can now be investigated. From Eq. (40):

$$a = \frac{Q_s}{T_s - T_p} \tag{43}$$

With substitution from Eq. (42), one obtains:

$$a = \frac{Q_s}{(T_u - T_p) - Q_s/b}$$

$$= \frac{Q_s}{(T_u - T_p) - Q_s/(\dot{V}_{si}(\rho_o T_o/T_u)\, C_p)} \tag{44}$$

For Test 23, Q_s = 230 kW; T_u = 474K; upper layer temperature (experimental substitute for T_s) = 126°C and the associated T_p = 39°C [see list following

Eq. (27)]; and $\dot{V}_{si}$ = 4.03 m^3/s. The value a = 2.64 kW/K is obtained, which is substituted in Eq. (39), together with the expression for h from Eq. (29) to determine the effective drop diameter for cooling, d_c [see Eq. (33)]. Values of u_p and u_s are taken as averages of values listed in Table IV over the distance from the sprinkler to the pseudodistance, x = 0.856 m (true distance $\delta_u - \delta_s$ = 1.00 m), where the calculation spray attains a radius of 1.73 m. Calculation of averages requires values at the location of the sprinkler ($x = x^* = 0$); consistent with the theory[2], the initial values of both u_p and u_s are set equal to u_{po}. (Average values calculated for u_p and u_s are 4.70 m/s and 1.02 m/s, respectively.) With the appropriate substitutions in Eq. (29), the effective drop size for cooling is calculated (iteratively) as $d_c = 0.336 \cdot 10^{-3}$ m for Test 23. This drop size may be compared to the volume mean diameter for the conditions of Test 23, calculated from Eq. (4) using the value of r in Eq. (35), i.e., $d = 0.627 \cdot 10^{-3}$ m. Using the definition in Eq. (33):

$$\zeta = d_c/d = 0.54$$

The other selected tests have been treated similarly. As in the case of Test 23, no penetration of the spray-induced jet into the lower layer was ever evident, and the calculated entrainment rate of lower layer fluid into the upper layer was always less than one percent of $\dot{V}_{si}$, i.e., the calculated flow rate associated with the spray induced jet in the upper layer at the layer interface.

Figure 7 presents all the ratios $\zeta = d_c/d$ calculated, plotted as a function of the heat release rate. The various data points are identified by their associated test numbers. The plot covers essentially three heat release rates, three discharge rates of the sprinklers, and two sprinkler sizes. It is observed that there is a slight decline in ζ with heat release rate, contrary to ideal behavior and the reason for which is not clear. The arithmetic mean of all determinations is:

$$\zeta = 0.70. \tag{45}$$

This level is indicated in the figure.

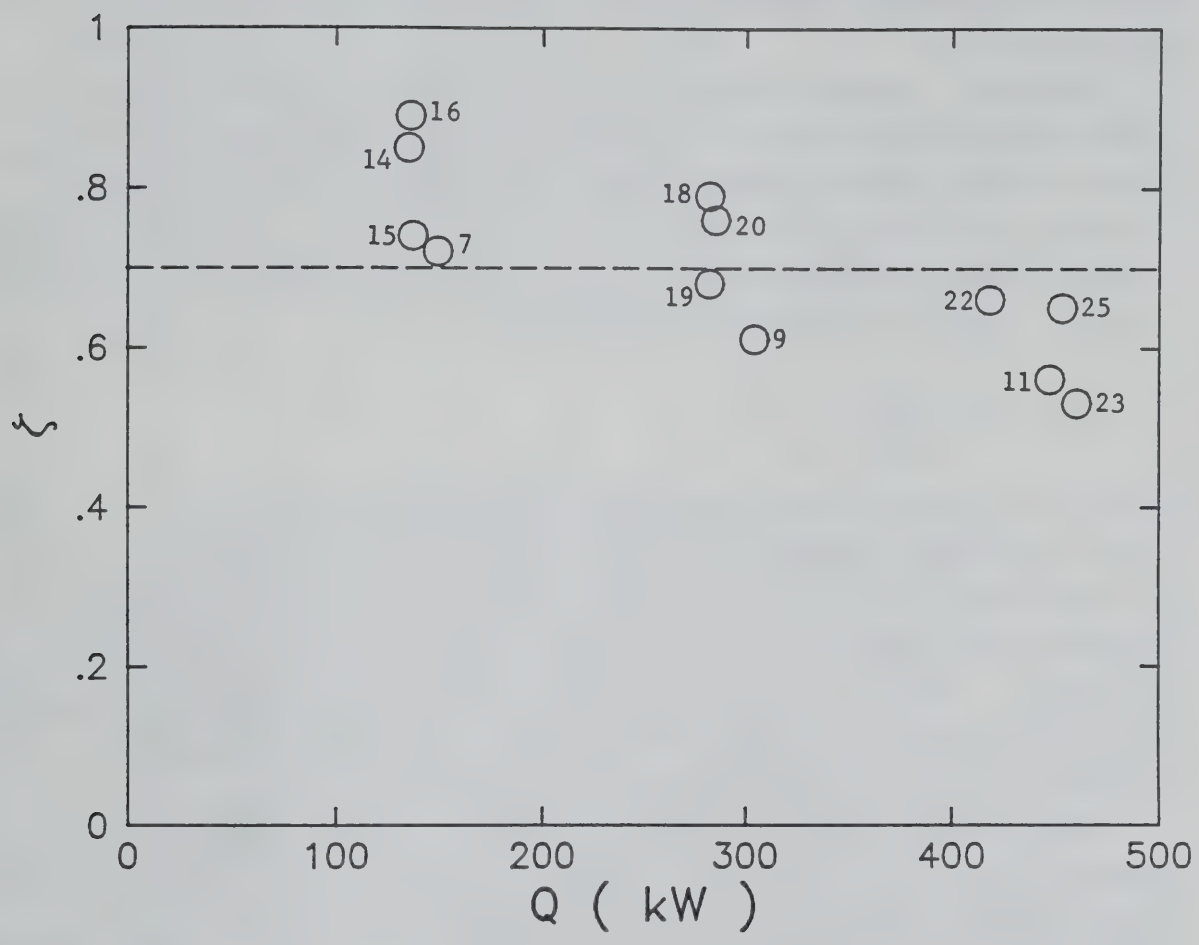

Figure 7. Ratios $\zeta = d_c/d$ indicated by experiments of You et al.[14], plotted as a function of the heat release rate.

The calculations represented in Figure 7 assume, it is recalled, that the drop temperature is the wet bulb temperature corresponding to the calculated gas temperature in the spray. Calculations assuming a drop temperature equal to the wet bulb temperature at the freeburn temperature have shown a slightly greater decrease of ζ with Q, whereas calculations assuming a drop temperature equal to the ambient temperature have indicated a dependence of ζ on Q similar to Figure 7.

Assuming ζ constant at the value in Eq. (45), one may now calculate the associated sprinkler cooling rates in the selected experiments and compare these with the directly measured rates. The effective drop diameter for cooling is calculated from Eqs. (45), (33), (8) and (35). Next, the value of a in Eq. (39) is calculated with the aid of Eq. (29), assuming T_s is unchanged from the previous calculations. From Eq. (37):

$$T_s = \frac{bT_u - aT_p}{a + b} \tag{46}$$

where b is unchanged from the previous calculations. Equation (46) is used to check the original assumption for T_s. If the new and original values differ, the new value for T_s is used in a new calculation of a. The procedure is continued until the value for T_s from Eq. (46) matches the assumption to calculate a. Finally, the cooling rate is calculated from Eq. (40), using the established values of a and T_s. The results of these calculations are presented in Figure 8 as Calculated Q_s versus Measured Q_s.

The procedure described above is acceptable since the final T_s does not differ greatly from the original assumption for T_s. The two values may differ significantly in a normal calculation of cooling rate in the intended application of this model. In that case, a trial value for T_s is first assumed, such as the freeburn temperature in the upper layer, associated values β and ξ evaluated, and then the equivalent of a table like Table IV prepared, yielding a first value for $\dot{V}_{si}$. This value for $\dot{V}_{si}$ allows b and a to be calculated and the first trial value of T_s to be checked. If the new and the trial values differ (as they probably always will), the new value is substituted as a second trial value and the procedure repeated a sufficient number of times that Eq. (46) confirms the last trial value.

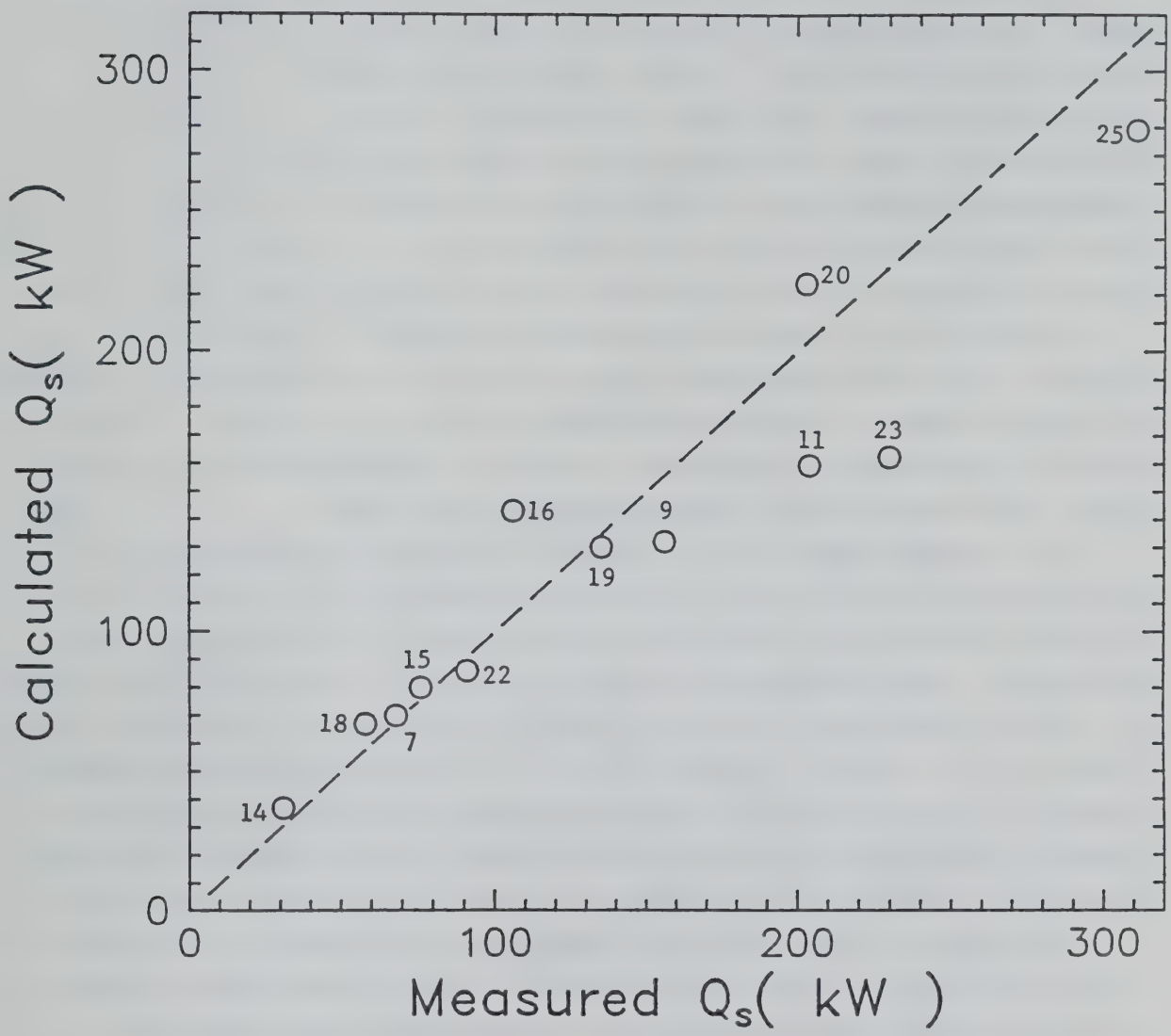

Figure 8. Comparison of calculated and experimental [14] spray cooling rates. (Test numbers indicated.)

IV

PENETRATION AND ENTRAINMENT BEHAVIOR

In Sections 2.2 and 2.3 it was concluded that applications of Turner's work(3) to the penetration behavior of the spray-induced jet into the lower layer and of Baines' work(4) to the associated entrainment of lower layer fluid into the upper layer had to be considered tentative. The reason for this caution is that there may possibly be significant effects of the spray traversing the penetrated fluid and of air entrained into the spray below the layer interface, which have not been accounted for in the model. Nevertheless, a few calculations with the predictive relations developed are instructive.

In Section 3.2, based on applications of Turner's(3) and Baines'(4) results, none of the experiments employed to verify the cooling model produced jet penetrations or significant entrainment from the lower layer. In this section, penetration and entrainment behavior is investigated using various upper layer depths and gas temperatures within the spray.

It is assumed that a 1/2 in. standard sprinkler is operating at the ceiling level (D = 0.437 in. = 11.1 mm), discharging at $\dot{V}_w = 1.89 \cdot 10^{-3}$ m^3/s (30 gpm) and producing a 120° spray over the range of ceiling layer depths considered. Other assumptions include: $C_M = 0.4$; $r = 0.065$ $m/s^{2/3}$; $\xi = 0.70$; $T_\ell = 20°C$. Associated quantities include $D_w = 0.0176$ m; $u_n = 19.6$ m/s; $u_{po} = 7.84$ m/s; $\beta_o = 1.99 \cdot 10^{-2}$; and $\xi_o = 4.57 \cdot 10^{-3}$. Entrainment tables were established, similar to Table IV, using appropriate values of β and ξ for each value of T_s selected. Equation (17) was used to calculate penetration depth and Eq. (26) was used to calculate entrainment rates from the lower layer.

The results of the penetration calculations are presented in Figure 9 as penetration depth δ_p versus the difference in temperature between the gas in the spray and the lower layer, $T_s - T_\ell$. Various smoke layer depths are represented: 0.35 m, 0.71 m, and 1.41 m. Except for the smallest depth, temperature differences are rather small for significant penetrations. Once penetration begins to occur as temperature differences decrease, the penetration depth increases rapidly with further decreases. (A penetration depth extending to the floor might be interpreted as a breakdown of the two layer model, with smoke dispersal throughout the enclosure volume.) Figure 10 presents associated volumetric entrainment rates from the lower layer

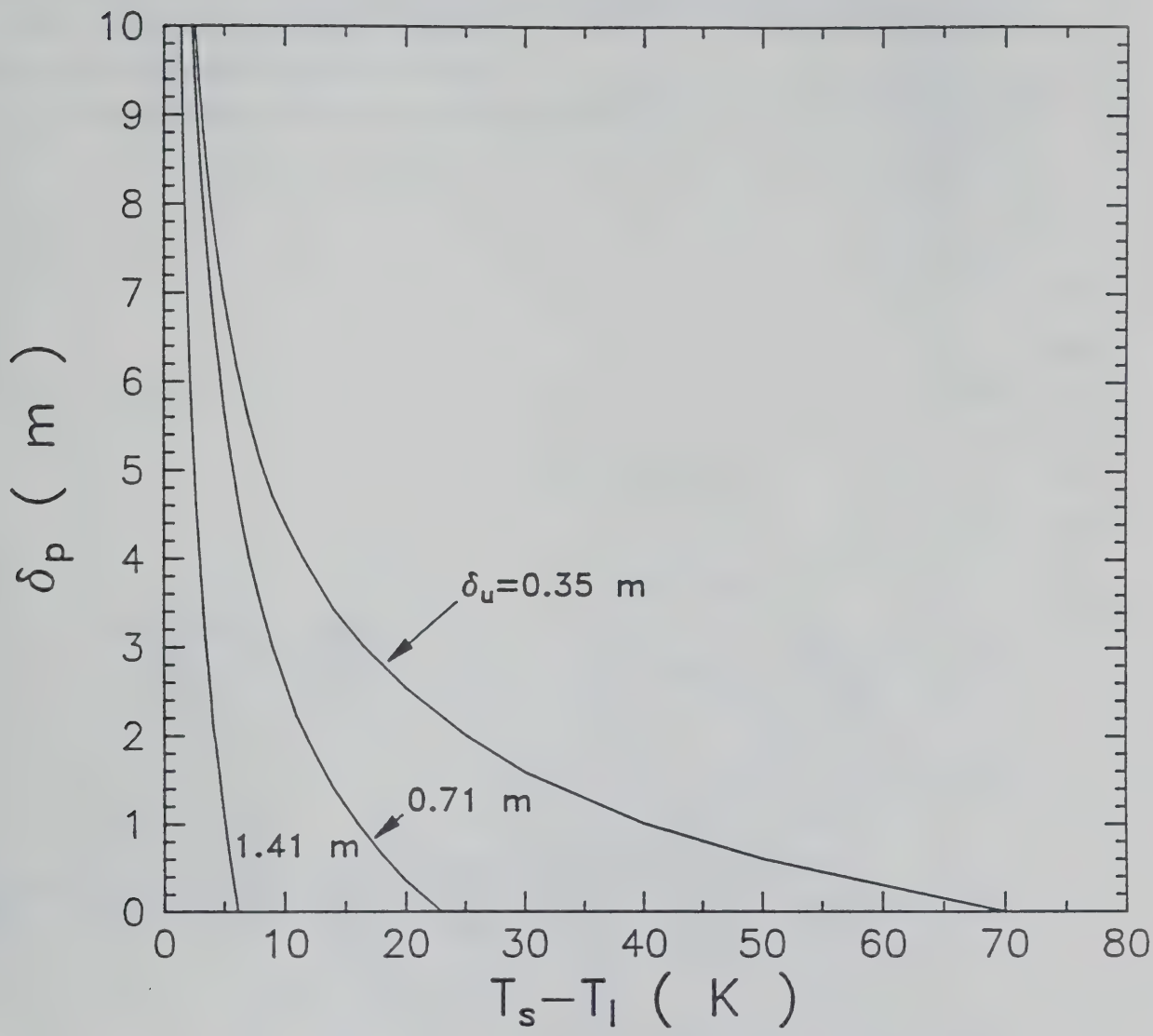

Figure 9. Influence of the temperature difference between gas in spray and lower layer on jet penetration depth beneath layer interface for various layer depths, δ_u. (1/2 in. standard sprinkler discharging 1.89 ℓ/s at ceiling level.)

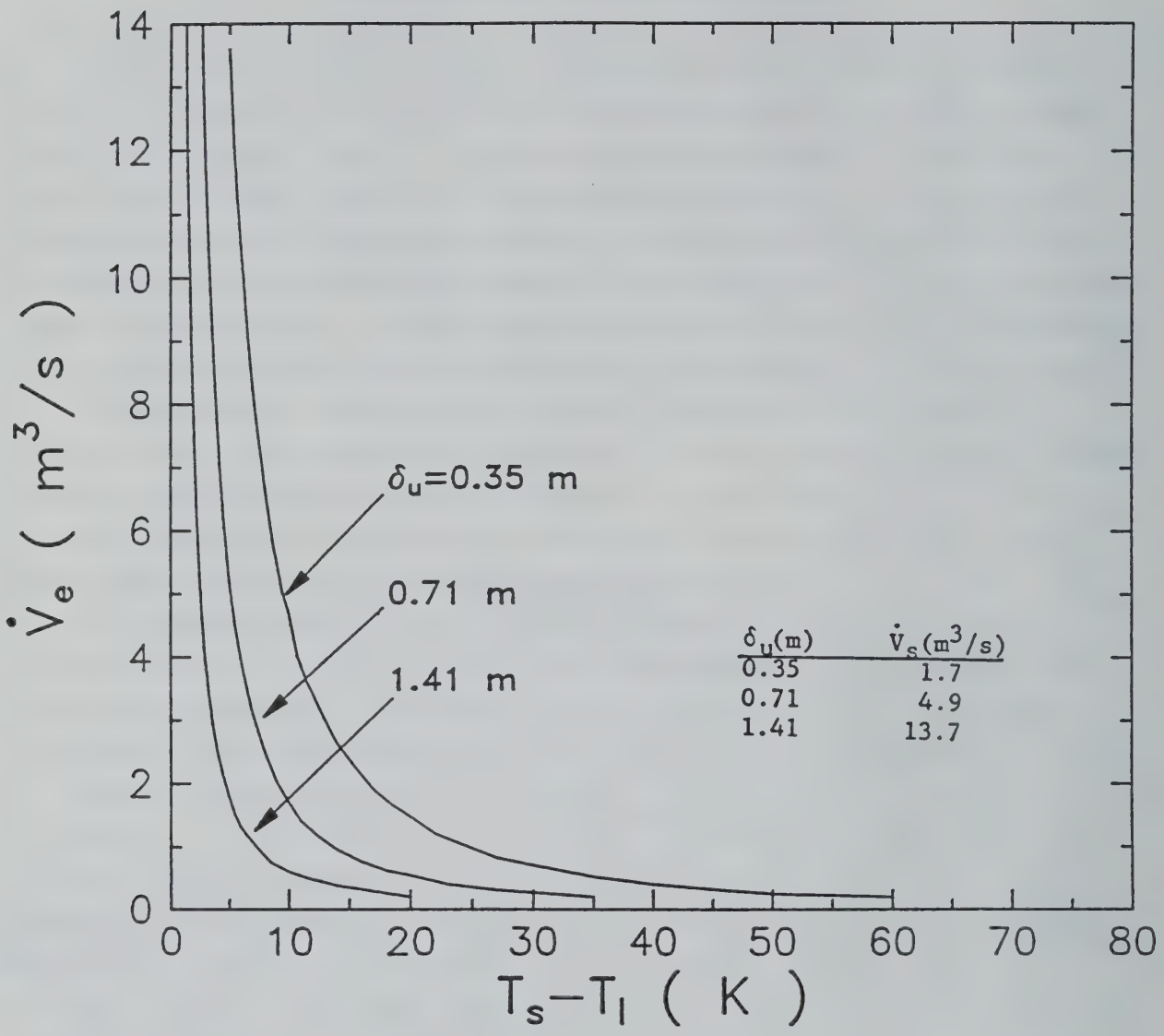

Figure 10. Volumetric entrainment rates from lower layer associated with Figure 9.

($\dot{V}_e$), including a brief table for reference showing entrained flow rates in the spray at the interface level ($\dot{V}_s$). Significant entrainment rates from the lower layer develop as the temperature differences between the gas in the spray and the lower layer is reduced.

No data have been found to test the predictions in Figures 9 and 10.

V

MODEL PARAMETERS

The following input parameters are indicated:

D sprinkler nozzle diameter (m)

$\dot{V}_w$ volumetric sprinkler discharge rate ($m^3\ s^{-1}$)

R_i spray radius at interface between upper and lower layers (m)

δ_u depth of upper layer (m)

δ_s distance of sprinkler below ceiling (m)

T_u upper layer temperature in absence of spray (K)

T_ℓ lower layer temperature (K)

C_M Momentum coefficient of sprinkler, with a typical value of 0.4.

r volume-mean drop size parameter, with a typical value of 0.084 $m \cdot s^{-2/3}$

ζ ratio of effective-cooling drop diameter to volume-mean drop diameter in spray, with a typical value of 0.70

Fixed input parameters include:

ν_o kinematic viscosity of air at room temperature ($1.49 \cdot 10^{-5}\ m^2\ s^{-1}$)

ρ_o density of air at STP (1.20 kg m^{-3})

ρ_w density of liquid water (1000 kg m^{-3})

g acceleration of gravity (9.81 m s^{-2})

T_r reference temperature (273 K)

The following output parameters have been recognized:

$\dot{V}_s$ volumetric spray-induced flow rate of gas in upper layer ($m^3\ s^{-1}$)

u_s spray induced downward gas velocity in upper layer (m s^{-1})

u_p drop velocity in upper layer (m s^{-1})

T_s average gas temperature within spray in upper layer (K)

Q_s heat absorption rate of water spray (kW)

$\dot{m}_e$ mass entrainment rate of gas from lower layer into upper layer, generated by spray-induced flow impinging on layer interface (kg s^{-1})

$\dot{m}_{ev}$ mass evaporation rate of water (kg s^{-1})

δ_p penetration depth of spray induced gas flow below layer interface (m)

VI

CONCLUSIONS

1. A model has been developed for the cooling of a fire-heated hot layer in a room by a sprinkler spray, based on existing models of spray generated flow and convective heat transfer coefficients for evaporating drops. The model assumes upper (hot) and lower (cool) layers of uniform temperatures and no direct spray interaction with a fire plume.

2. The cooling model has been augmented with models for penetration of the spray-induced hot-layer jet into the lower layer and associated entrainment of lower-layer fluid into the upper layer, based on previous studies with momentum driven jets and buoyant plumes. It is cautioned that these models are tentative because of possible effects of the spray on the penetrating fluid. According to these models, significant penetration and entrainment from the lower layer occurs only at low hot layer temperatures (compared to typical temperature ratings of sprinklers), with greatest effects for shallow hot layers.

3. The cooling model has been tested against published results from sprinklered room-fire experiments, where the hot layer depth was about 1.0 m below the sprinkler. Good agreement was observed under various conditions, which included two sprinkler sizes, three water discharge rates and three heat release rates, although a segment of the sprinkler spray intercepted the fire plume. The effective cooling diameter of the drops in the spray was indicated at 70% of the volume-mean diameter.

4. Calculated penetration depths and associated entrainment rates from the lower layer were insignificant in all experiments referred to in the preceding conclusion. No data were available from the experiments to verify these calculations. Furthermore, no other data have been found to test the penetration and associated entrainment predictions in sprinkler/hot layer situations.

REFERENCES

1. Heskestad, G., Kung, H-C. and Todtenkopf, N.F., "Air Entrainment into Water Sprays and Spray Curtains," ASME Paper 76-WA/FE-40, American Society of Mechanical Engineers, 1976.

2. Heskestad, G., Kung, H-C. and Todtenkopf, N.F., "Air Entrainment into Water Sprays," RC77-TP-7, Factory Mutual Research Corporation, November 1977.

3. Turner, J.S., "Jets and Plumes with Negative or Reversing Buoyancy," J. Fluid Mech., 26 (1966), pp. 779-792.

4. Baines, W.D., "Entrainment by a Plume or Jet at a Density Interface," J. Fluid Mech., 68 (1975), pp. 309-320.

5. Yuen, M.C. and Chen, L.W., "Heat-Transfer Measurements of Evaporating Liquid Drops," J. Heat Mass Transfer, 21 (1978), pp. 537-542.

6. Bullen, M.L., "The Effect of a Sprinkler on the Stability of a Smoke Layer Beneath a Ceiling," Fire Research Note No. 1016, Fire Research Station, Borehamwood, July 1974.

7. Morgan, H.P., "Heat Transfer from a Buoyant Smoke Layer Beneath a Ceiling to a Sprinkler Spray. 1 - A Tentative Theory," Fire and Materials, 3 (1979), pp. 27-32.

8. Morgan, H.P. and Baines, K., "Heat Transfer From a Buoyant Smoke Layer Beneath a Ceiling to a Sprinkler Spray. 2 - An Experiment," Fire and Materials, 3 (1979), pp. 34-38.

9. Heselden, A.J.M., "The Interaction of Sprinklers and Roof Venting in Industrial Buildings: The Current Knowledge," Report BR57, Building Research Establishment, Borehamwood, 1984.

10. Hinkley, P.L., "The Effect of Smoke Venting on the Operation of Sprinklers Subsequent to the First," Fire Safety Journal, 14 (1989), pp. 221-240.

11. Turner, J.S., Personal Communication, The Australian National University, Canberra, April 10, 1990.

12. Ricou, F.P. and Spalding, D.B., "Measurements of Entrainment by Axisymmetrical Turbulent Jets," J. Fluid Mech., 11 (1961), p. 21.

13. Yuen, M.C. and Chen, L.W., "On Drag of Evaporating Liquid Drops," Combustion Science and Technology, 14 (1976), pp. 147-154.

14. You, H-Z., Kung, H-C., and Han, Z., "Spray Cooling in Room Fires," Twenty-First Symposium (International) on Combustion, The Combustion Institute, Pittsburgh, Pennsylvania, 1986, pp. 129-136.

15. You, H-Z., Kung, H-C., and Han, Z., "The Effects of Spray Cooling on the Ceiling Gas Temperature at the Door Opening of Room Fires," Fire Safety Science-Proceedings of the Second International Symposium, Hemisphere, New York, 1989, pp. 655-665.

16. Yu, H-Z., Personal Communication, Factory Mutual Research Corporation, Norwood, MA, August 1990.

17. Thomas, P.H., "Studies of Fires in Buildings Using Models," Research, 13 (1960), p. 87.

18. You, H-Z., Kung, H-C., and Han, Z., "Spray Cooling in Room Fires," FMRC J.I.0J0N9.RA, Factory Mutual Research Corporation, Norwood, MA, March 1986.

SYMBOLS

A	Cross sectional area of spray
a	defined in Eq. (39)
B	constant in Eqs. (2) and (3)
b	defined in Eq. (38)
b_1	local radius to 0.368 times centerline velocity in plume or jet
C_M	ratio of initial spray momentum to flow momentum in nozzle
C_p	specific heat of air at constant pressure
D	nozzle diameter
D_w	effective initial spray diameter; see Eq. (7)
d	drop diameter, or volume mean drop diameter in polydisperse spray
Fr	Froude number; see Eq. (15)
Fr_G	Froude number, see Eq. (20)
f	$1.16 \cdot 10^{-4} K^{-1.19}$, a constant
g	acceleration of gravity
h	convective heat transfer coefficient
h_n	distance from ceiling to neutral plane
k_o	thermal conductivity of air at room temperature
L_w	latent heat of vaporization of water
M	local momentum flux in impinging jet
$\dot{m}_e$	mass entrainment rate from lower layer into upper layer
$\dot{m}_{ev}$	mass addition rate of water vapor to upper layer
Q_a	actual heat release rate
Q_c	convective heat release rate
Q_s	heat absorption rate of spray
Q^*	$\dot{V}_s/\dot{V}_w$, nondimensional entrained flow in spray
R	spray or nozzle radius
R^*	R/D_w, nondimensional spray radius
R_i	spray radius at interface level
r	drop size parameter defined in Eq. (8)
T_a	air temperature
T_f	$(T_u + T_p)/2$, film temperature
T_ℓ	lower layer temperature
T_o	room temperature (20°C)

T_p	drop temperature
T_r	273K, a reference temperature
T_s	gas temperature within spray
T_u	temperature of upper layer
T_∞	ambient temperature
ΔT	temperature rise
ΔT_b	bulk temperature rise of fire gases leaving room
u	velocity
u_a	air velocity
u_n	nozzle discharge velocity
u_p	drop velocity
u_{po}	initial drop velocity
u_s	gas velocity within spray
u_{si}	u_s at interface level
u_p^*	u_p/u_{po}, nondimensional drop velocity
$\dot{V}_e$	volumetric entrainment rate from lower (heavier) layer into upper (lighter) layer
$\dot{V}_s$	volumetric gas flow rate in spray
$\dot{V}_{si}$	$\dot{V}_s$ at interface level
$\dot{V}_w$	volumetric water discharge rate of spray nozzle
w_1	centerline velocity of plume or jet (in Baines' model)
x	distance below spray nozzle
x^*	x/D_w, nondimensional distance below spray nozzle
z	distance below ceiling
β	viscous interaction parameter; see Eq. (2)
β_o	β evaluated at room temperature
γ	geometric parameter, see Eq. (1)
γ_o	γ evaluated at room temperature
δ_p	penetration depth of jet
δ_s	distance of sprinkler below ceiling
δ_u	depth of upper layer
ζ	constant of proportionality, see Eq. (33)
η	constant
θ	conical spray angle
μ_o	dynamic viscosity of air at room temperature

ν	kinematic viscosity of air
ξ	gravity parameter; see Eq. (3)
ξ_o	ξ evaluated at room temperature
ρ	density of gas (essentially air)
ρ_o	density of air at STP
ρ_1	density of jet fluid
ρ_2	density of heavier fluid
ρ_{ao}	density of lighter fluid
ρ_ℓ	density of lower layer
ρ_s	density of gas within spray
ρ_w	density of water
$\Delta\rho$	density difference

NIST-114A
(REV. 3-90)

U.S. DEPARTMENT OF COMMERCE
NATIONAL INSTITUTE OF STANDARDS AND TECHNOLOGY

BIBLIOGRAPHIC DATA SHEET

1. PUBLICATION OR REPORT NUMBER
NIST-GCR-91-590

2. PERFORMING ORGANIZATION REPORT NUMBER

3. PUBLICATION DATE
May 1991

4. TITLE AND SUBTITLE
Sprinkler/Hot Layer Interaction

5. AUTHOR(S)
Gunnar Heskestad

6. PERFORMING ORGANIZATION (IF JOINT OR OTHER THAN NIST, SEE INSTRUCTIONS)
Factory Mutal Research Corporation
1151 Boston-Providence Turnpike
Norwood, MA 02062

7. CONTRACT/GRANT NUMBER
60NANB0D1006

8. TYPE OF REPORT AND PERIOD COVERED
Technical Report/Sept. 1990

9. SPONSORING ORGANIZATION NAME AND COMPLETE ADDRESS (STREET, CITY, STATE, ZIP)
U.S. DEPARTMENT OF COMMERCE
National Institute of Standards
and Technology
Gaithersburg, MD 20899

10. SUPPLEMENTARY NOTES

11. ABSTRACT (A 200-WORD OR LESS FACTUAL SUMMARY OF MOST SIGNIFICANT INFORMATION. IF DOCUMENT INCLUDES A SIGNIFICANT BIBLIOGRAPHY OR LITERATURE SURVEY, MENTION IT HERE.)

A model has been developed for the cooling of a quiescent hot layer by a sprinkler spray in a two-layer zone model (with no direct interaction of the spray with a fire plume), based on existing models of spray-induced flow and heat transfer to evaporating drops. In addition, existing models have been adapted to predict the penetration of the spray-induced flow below the layer interface and associated entrainment of lower-layer fluid into the upper layer. The cooling model is in good agreement with published results from sprinklered room-fire experiments, for which penetration of spray-induced flow into the lower layer and associated entrainment were calculated to be negligible. No published results have been found to test the validity of the adapted models of penetration and associated entrainment, which do not account for possible effects of the spray below the layer interface.

12. KEY WORDS (6 TO 12 ENTRIES; ALPHABETICAL ORDER; CAPITALIZE ONLY PROPER NAMES; AND SEPARATE KEY WORDS BY SEMICOLONS)

13. AVAILABILITY

X	UNLIMITED
	FOR OFFICIAL DISTRIBUTION. DO NOT RELEASE TO NATIONAL TECHNICAL INFORMATION SERVICE (NTIS).
	ORDER FROM SUPERINTENDENT OF DOCUMENTS, U.S. GOVERNMENT PRINTING OFFICE, WASHINGTON, DC 20402.
X	ORDER FROM NATIONAL TECHNICAL INFORMATION SERVICE (NTIS), SPRINGFIELD, VA 22161.

14. NUMBER OF PRINTED PAGES
55

15. PRICE
A04

ELECTRONIC FORM